Proceedings of the 35th Chinese Control Conference
July 27-29, 2016, Chengdu, China

Effect of Variation in Rotor Resistance on the Dynamic Performance of Induction Motor

Athar Hanif[1], S.M.Nawazish Ali[1], Qadeer Ahmed[2], A. I. Bhatti[3], Guodong Yin[4] and Mujtaba H Jaffery[1]

1. Department of Electrical Engineering, COMSATS Institute of Information Technology, Lahore 54000, I. R. Pakistan
E-mail: athar.hanif@ciitlahore.edu.pk,nawazishali@ciitlahore.edu.pk,m.jaffery@ciitlahore.edu.pk

2. Centre for Automotive Research (CAR), The Ohio State University, Ohio 43210, USA
E-mail: qadeer62@gmail.com

3. Department of Electrical Engineering, Capital University of Science and Technology, Control and Signal Processing Research Group (CASPR), Islamabad 75400, I. R. Pakistan
E-mail: aamer987@gmail.com

4. School of Mechanical Engineering, Southeast University, Nanjing 211189, China
E-mail: ygd@seu.edu.cn

Abstract: The paper presents a dynamic d-q model of the three-phase induction motor in the stationary reference frame using MATLAB Simulink environment. An intuitive and easy to use model is presented that clearly elaborates the steps regarding revolving reference frames. It gives a complete access to the monitoring of parameters of induction motor for verification and control purposes. The second part of the paper comprises of the effect of variation in rotor resistance on the dynamic performance of induction motor using the same model. Extensive nonlinear simulation results are incorporated that clearly elaborates the change in the dynamic performance of induction motor by changing the rotor resistance which becomes dominant due to temperature rise in motor.

Key Words: d-q model, dynamic performance, induction motor, nonlinear simulation, rotor resistance variation

1 Introduction

One of the core requirements of an industrial plant is induction motor. With the advancements in power electronics, the induction motor usage has been increased from being a constant speed motor to a variable speed motor [1]. Three phase induction motors found many applications in driving units of compressors, fans and pumps. The induction motor drives can be immensely found in onboard submarines, in various mining operations, commercial jet planes and Hybrid Electric Vehicles (HEV) applications.

Its extensive applications have made it quite significant to study the control of high performance induction motors for which motor modeling is the foremost requirement. Usually, only the steady state model of motor is used in simulators like PSpice whereas in order to control various parameters affecting the performance, transient model should be considered. Simulation of transient model of induction motor plays a significant role in pre-testing of the motor drive systems [2].

As far as the transient modeling equations are known, any type of control algorithm can be implemented in Simulink environment. Two approaches usually used for modeling are by using S-function and by using Simulink Power System Blockset [3]. Both of these techniques demand additional expense and intensive programming due to which they are not easy to handle.

In this paper, a MATLAB Simulink based transient model of induction motor is described with meticulous details of each subsystem. The values of controlling parameters along with the simulation results are also discussed. Moreover, the effect of variation in rotor resistance on the dynamic model of induction motor is also explained accompanying with the simulation results.

In view of significant factors such as reliability, controllability, simplicity and cost, induction motor is superior to synchronous motor, switched reluctance motor and DC motor. Hence it is the most suitable electric motor for automotive applications [4], [5], [6]. One of the significant parameter that is responsible for the variations in the dynamic performance of induction motor is its rotor resistance. The variation in rotor resistance of motor cause a considerable change in its torque-speed characteristics. All of the motor applications require a proper value of torque and speed for their working [7]. The variation in rotor resistance due to temperature rise is the main cause of change in torque of motor. This paper includes the nonlinear simulation results for the variation in dynamic behavior of the nonlinear model of induction motor due to the change in rotor resistance.

2 Dynamic Model of Induction Motor

The induction motor direct-quadrature (d-q) dynamic model is derived from the circuits represented in the stationary reference frame shown in Figs. 1 and 2. The idea is to decouple the flux and torque components that are incipiently coupled and both of them are the functions of current or voltage [8]. Assuming the induction motor is of squirrel cage type, d-q rotor voltages leads to zero [9]. The following four differential equations are extracted from the d-q equivalent circuits:

$$\begin{aligned}\frac{d}{dt}i_{ds} &= -\frac{(L_m^2R_r + L_r^2R_s)}{\sigma L_s L_r^2}i_{ds} + \frac{L_mR_r}{\sigma L_s L_r^2}\psi_{dr} \\ &+ n_p\frac{L_m\omega_r}{\sigma L_s L_r}\psi_{qr} + \frac{1}{\sigma L_s}V_{ds}^2 \qquad (1)\end{aligned}$$

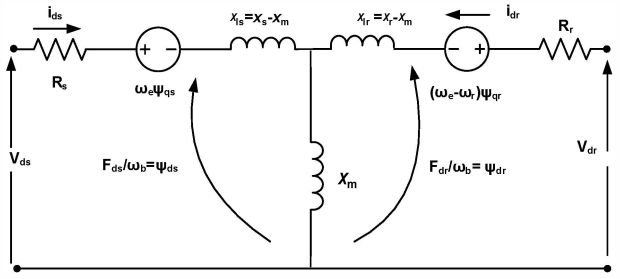

Fig. 1: Direct axis equivalent circuit

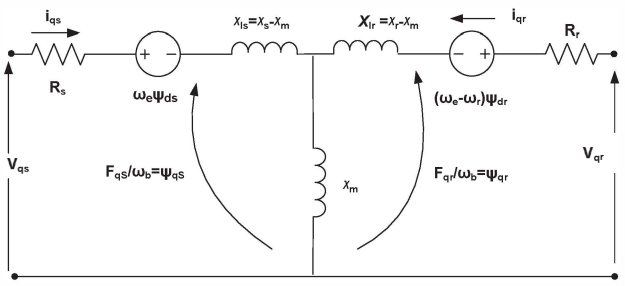

Fig. 2: Quadrature axis equivalent circuit

$$\begin{aligned}\frac{d}{dt}i_{qs} &= -\frac{(L_m^2R_r + L_r^2R_s)}{\sigma L_s L_r^2}i_{qs} + \frac{L_mR_r}{\sigma L_s L_r^2}\psi_{qr} \\ &- n_p\frac{L_m\omega_r}{\sigma L_s L_r}\psi_{dr} + \frac{1}{\sigma L_s}V_{qs}^2 \end{aligned} \quad (2)$$

where

$$\sigma = 1 - \frac{L_m^2}{L_sL_r}$$

$$\frac{d}{dt}\psi_{dr} = -\frac{R_r}{L_r}\psi_{dr} - n_p\omega_r\psi_{qr} + \frac{L_mR_r}{L_r}i_{ds} \quad (3)$$

$$\frac{d}{dt}\psi_{qr} = -\frac{R_r}{L_r}\psi_{qr} + n_p\omega_r\psi_{dr} + \frac{L_mR_r}{L_r}i_{qs} \quad (4)$$

$$\tau_e = \frac{3}{2}n_p\frac{L_m}{L_r}(\psi_{dr}i_{qs} - \psi_{qr}i_{ds}) \quad (5)$$

$$\frac{d}{dt}(\omega_r) = \frac{\tau_e}{J} - \frac{B}{J}\omega - \frac{\tau_L}{J} \quad (6)$$

The description of parameters used in the above equations is given in Table 1. The differential equations clearly elaborate the five states of nonlinear model of induction motor i.e. d-q stator currents (i_{ds},i_{qs}), d-q rotor fluxes (ψ_{dr},ψ_{qr}) and rotor angular velocity (ω_r). The inputs are three-phase voltages (V_{an},V_{bn} and V_{cn}) and the disturbance is in the form of load torque (τ_L). The outputs are three phase currents (i_a,i_b and i_c), electromagnetic torque (τ_e) and rotor angular velocity (ω_r) [10].

3 Simulink Model of Induction Motor

A three-phase squirrel cage induction motor model is used for simulation. The main Simulink system is shown in Fig. 3. It comprises of the following modules:

Table 1: Parameters of the Dynamic Model of Induction Motor

Parameter	Description	Units
F_{ds}	d-axis stator flux linkage	Wb
F_{qs}	q-axis stator flux linkage	Wb
F_{dr}	d-axis rotor flux linkage	Wb
F_{qr}	q-axis rotor flux linkage	Wb
V_{ds}	d-axis stator voltage	V
V_{qs}	q-axis stator voltage	V
i_{ds}	d-axis stator current	A
i_{qs}	q-axis stator current	A
ψ_{dr}	d-axis rotor flux	Wb
ψ_{qr}	q-axis rotor flux	Wb
L_s	stator self inductance	H
L_r	rotor self inductance	H
L_m	magnetizing inductance	H
R_r	rotor resistance	Ω
R_s	stator resistance	Ω
n_p	number of poles	
τ_e	electromagnetic torque	N-m
τ_L	load torque	N-m
ω_e	reference frame angular velocity	rad/s
ω_r	rotor angular velocity	rad/s
ω_b	base angular velocity	rad/s
J	moment of inertia of the rotor and connected load	kg-m^2
B	damping coefficient	N-m-s/rad

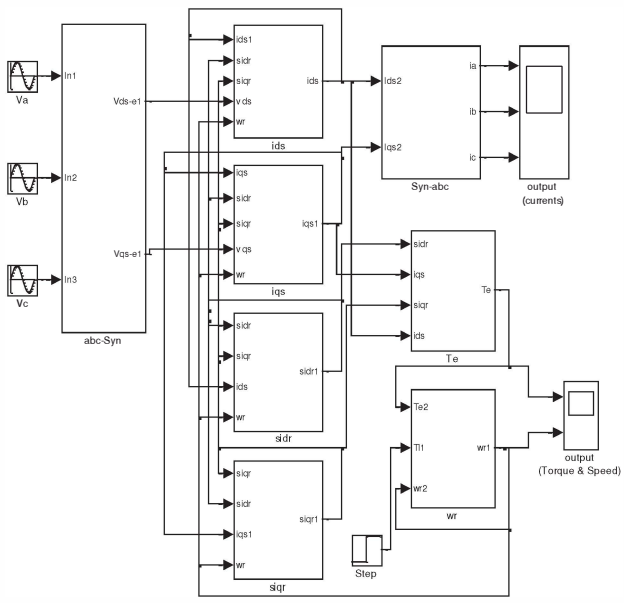

Fig. 3: Simulink model of induction motor

3.1 abc-stationary conversion module

In module 1, the three phase voltages are transformed into two phase d-q stator voltages in stationary frame [11] using the equation (7). This module is based upon the subsystem that is shown in Fig. 4.

$$\begin{bmatrix} V_{qs} \\ V_{ds} \end{bmatrix} = \begin{bmatrix} 1 & 0 & 0 \\ 0 & -1/\sqrt{3} & 1/\sqrt{3} \end{bmatrix} \begin{bmatrix} V_{an} \\ V_{bn} \\ V_{cn} \end{bmatrix} \quad (7)$$

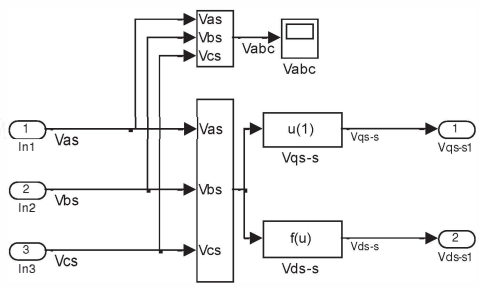

Fig. 4: Subsystem implementing (8) in Simulink

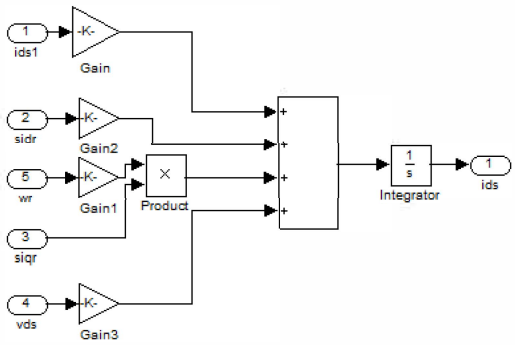

Fig. 5: Subsystem implementing (1) in Simulink

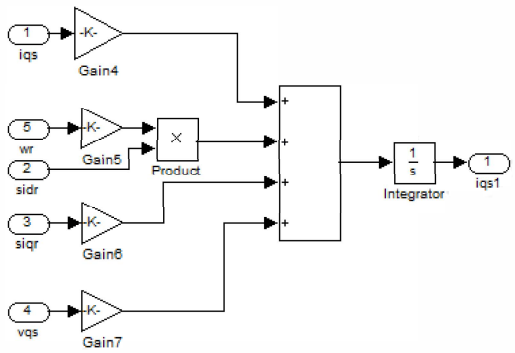

Fig. 6: Subsystem implementing (2) in Simulink

3.2 d-q stator currents and rotor fluxes module

Module 2 comprises of four subsystems representing four states of the nonlinear model of induction motor. They are developed using the equations (1), (2), (3) and (4). These subsystems are shown in Figs. 5,6,7 and 8.

3.3 Stationary-abc conversion module

Module 3 takes inputs as i_{qs} and i_{ds} from the previous module and convert them into three phase currents which act as an output of induction motor model using equation(8). This block is based upon the subsystem that is shown in Fig. 9.

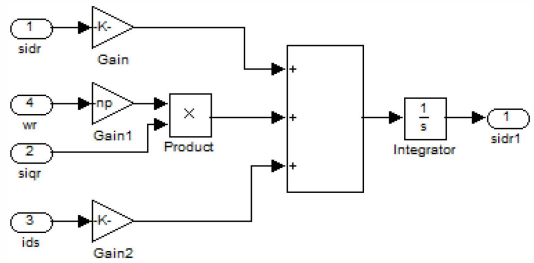

Fig. 7: Subsystem implementing (3) in Simulink

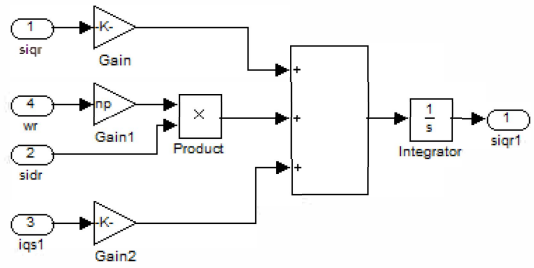

Fig. 8: Subsystem implementing (4) in Simulink

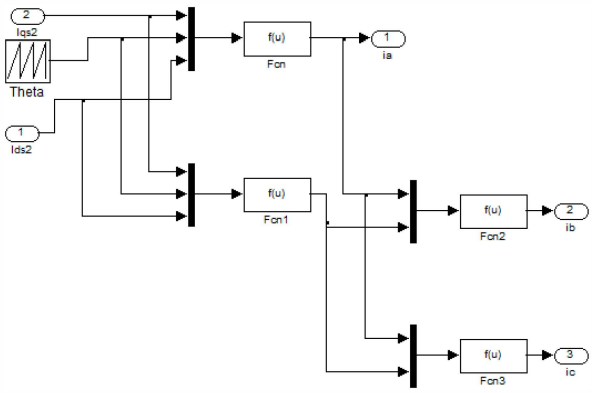

Fig. 9: Subsystem implementing (9) in Simulink

$$\begin{bmatrix} i_a \\ i_b \\ i_c \end{bmatrix} = \begin{bmatrix} 1 & 0 \\ -1/2 & -\sqrt{3}/2 \\ -1/2 & \sqrt{3}/2 \end{bmatrix} \begin{bmatrix} i_{qs} \\ i_{ds} \end{bmatrix} \tag{8}$$

3.4 Torque-speed modules

Module 4 comprises of two blocks. One is used for the generation of electromagnetic torque. This block is based upon the subsystem that is shown in Fig. 10. The second block is used to produce rotor angular velocity of induction motor. This block is based upon the subsystem that is shown in Fig. 11.

4 Model Simulation Results

In this section, MATLAB simulation results of each subsection of nonlinear induction motor model has been presented. Also the simulation results for the effect of variation

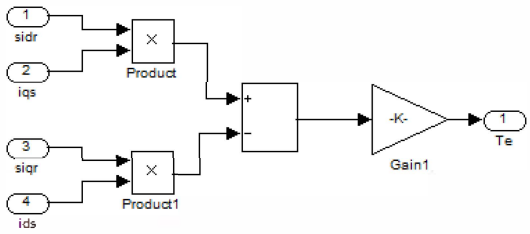

Fig. 10: Subsystem implementing (6) in Simulink

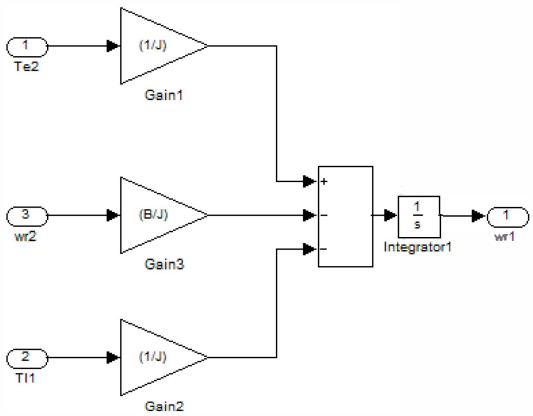

Fig. 11: Subsystem implementing (7) in Simulink

in rotor resistance on induction motor dynamic performance has been discussed.

4.1 Initialization

In order to simulate the dynamic model given in Fig. 3. , we first need to assign mathematical values to input parameters for which an m-file needs to be created in MATLAB. The values of input parameters are given in Table 2. The advantage of using m-file is the freedom of varying the values of motor parameters as per required in an easy and understandable way.

Table 2: Input Parameters of the Induction Motor Model

Parameter	Value/Formula
P	30kW
n_p	4
Rs	0.22 Ω
Rr	0.209 Ω
Ls	0.0425 H
Lr	0.043 H
Lm	0.04 H
B	0.01 N-m-s/rad
J	0.124 kg-m^2
σ	1-((Lm*Lm)/(Ls*Lr))
f	50 Hz
ω_e	2*pi*f

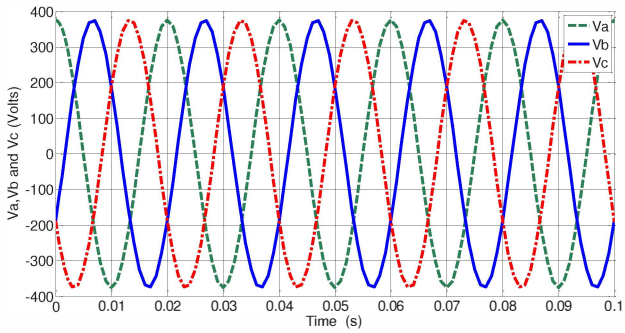

Fig. 12: Input voltages of induction motor

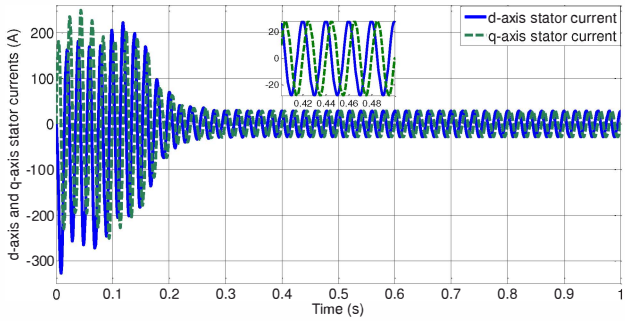

Fig. 13: d-q axis stator currents

4.2 Simulation plots

The three phase input voltages to the motor model are shown in Fig. 12. The simulation results of two states i.e. d-q axis stator currents are shown in Fig. 13 where as of other two states i.e. d-q axis rotor fluxes are given in Fig. 14. Another significant input to the motor model is load torque on which the rotor angular speed, electromagnetic generated torque and output currents depend. It simulation is shown in Fig. 15. It is obvious from Fig. 16 that as the load torque (τ_L) increases at t=1s, the rotor angular velocity (ω_r) decreases and similarly at t=1.5s, as τ_L decreases, there occurs an increase in ω_r. The simulation results validate the accuracy of the already described dynamic model of induction motor and hence it can be used to study various effects on induction motor.

The effect of load torque can also be seen in a particular phase of the output currents as shown in the zoomed portion of Fig. 17. At t=1s, as the load torque increases, there occurs an increase in the amplitude of output current waveform of a particular phase where as in the vicinity of t=1.5s, there occurs a decrease in the amplitude of output waveform as the load torque decreases.

4.3 Bi-polar load torque

Another form of load torque i.e. bi-polar square wave is applied to the motor model and variations in output parameters are shown in simulation graphs. Such type of τ_L incorporates the motoring effect for $0.5 \leq t \leq 1$ and the generating effect for $2 \leq t \leq 2.5$ as shown in Fig. 18. It is obvious from Fig. 19 that at points t=0.5s and t=2.5s, the plot of τ_L experiences a rising edge so the plot of ω_r experiences a falling edge. Similarly, at points t=1s and t=2s, the plot of τ_L experiences a falling edge so the plot of ω_r experiences a rising edge. This again validates the accuracy of the already de-

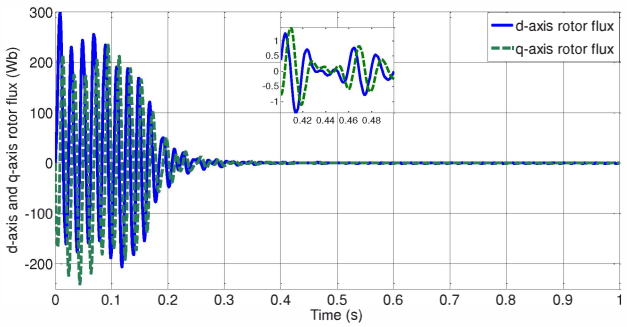

Fig. 14: d-q axis rotor fluxes

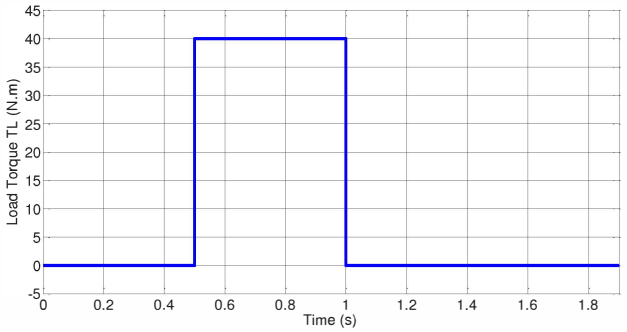

Fig. 15: Unipolar load torque

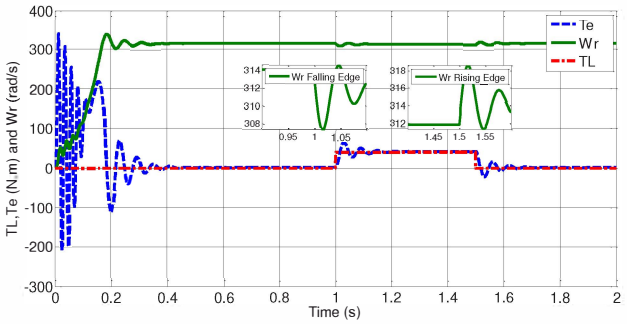

Fig. 16: Effect of unipolar load torque on rotor angular velocity

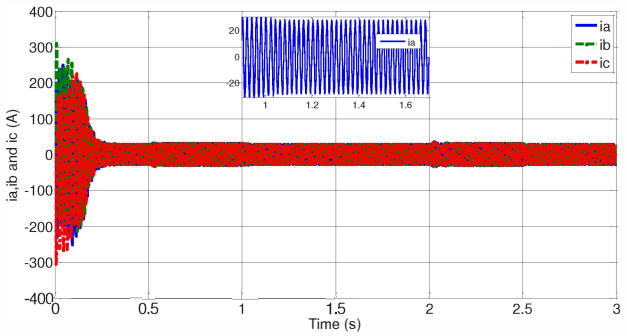

Fig. 17: Output currents corresponding to unipolar load torque

scribed induction motor model. The output currents in this case are shown in Fig. 20. It is clear from the figure that at t=0.5s, the τ_L experiences a rising edge due to which the amplitude of output current also increases and at t=1.0s, the τ_L experiences a falling edge due to which the amplitude of output current also decreases. Similarly, at t=2.0s, the τ_L

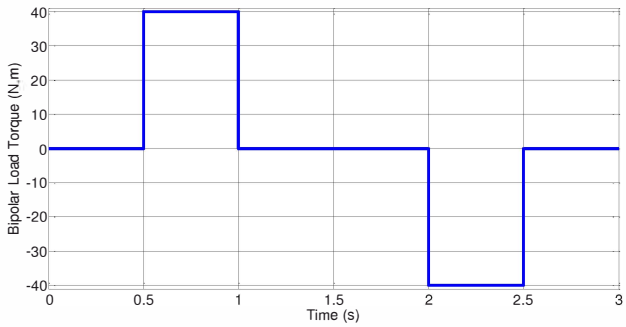

Fig. 18: Bipolar square wave load torque

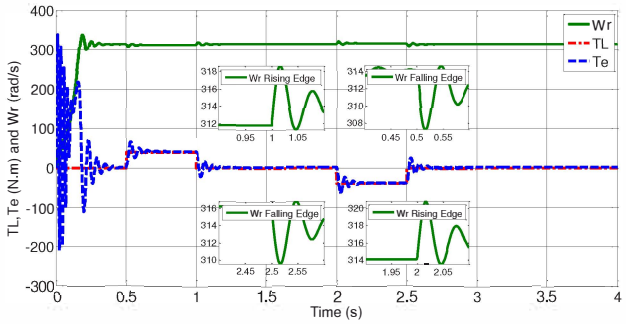

Fig. 19: Effect of bipolar load torque on rotor angular velocity

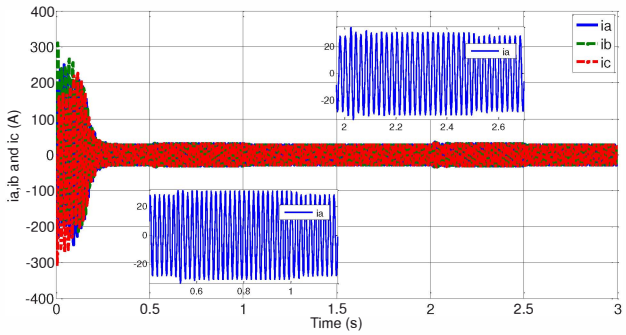

Fig. 20: Output currents corresponding to bipolar load torque

experiences a rising edge in opposite direction due to which the amplitude of output current also increases and at t=2.5s, the τ_L experiences a falling edge in opposite direction due to which the amplitude of output current also decreases.

4.4 Effect of variation in rotor resistance on induction motor dynamic performance

The torque-speed characteristic curves of induction motor depend upon the rotor resistance [12]. At a high value of rotor resistance, the starting torque and the slip of the motor is also quite high which results in the decrease in the amount of power in air-gap that actually converts into mechanical form. This phenomenon ultimately ends up with a lower efficiency of induction motor [13]. The described dynamic model of motor is simulated for three different values of rotor resistance which are given in Table 3. The simulation results are shown for both types of load torques discussed above in Figs 21 and 22.

In Fig. 21, the zoomed portions of the plot represent the variation in dynamic performance of induction motor model

Table 3: Values of Rotor Resistance

Rotor Resistance (R_r)	Value
half R_r	0.1045Ω
nominal R_r	0.209Ω
double R_r	0.418Ω

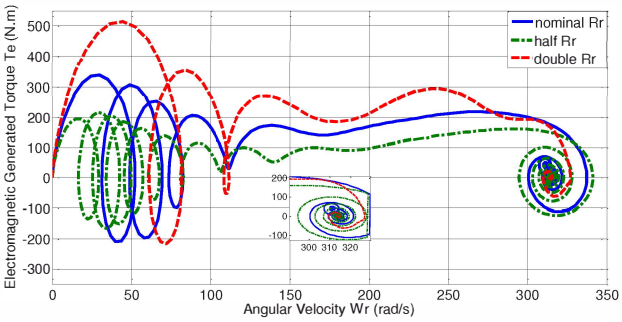

Fig. 21: Effect of variation in rotor resistance for unipolar load torque

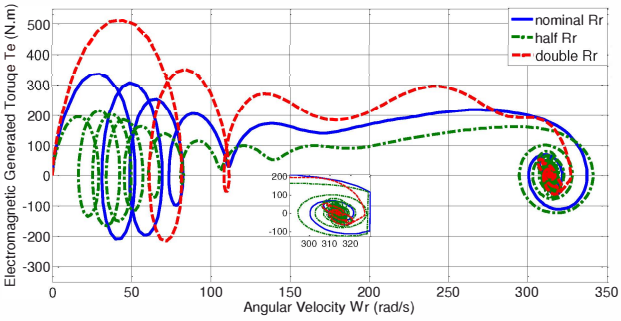

Fig. 22: Effect of variation in rotor resistance for bipolar load torque

by the change in rotor resistance. It can be observed in the zoomed graph of nominal rotor resistance that there are two steady state points which are due to the effect of load torque having two transitions as already shown in Fig. 15. Similarly, in case of bi-polar load torque, there are three steady state points as shown in the zoomed graphs of Fig. 22. The values of Electromagnetic generated torque and rotor angular velocity are significantly effected by the variation in rotor resistance.

5 Conclusion

A Simulink based induction motor's dynamic model is presented. Simulink block model methodology is used to develop the model of the motor in such a way that it addresses all the issues regarding the stationary reference frame. The model can be used for the flux estimation techniques, power inverter topologies and in induction motor drives with minor changes. The effect of variation in rotor resistance on the described dynamic model is also presented along with simulation results for nominal, below nominal and above nominal values of rotor resistance. Significant variations in the dynamic performance of induction motor are observed on changing the rotor resistance.

Acknowledgment

Authors are grateful to the Center for Automotive Research (CAR), The Ohio State University, Columbus, U.S.A for providing the research directions. Also appreciate the department of Electrical Engineering COMSATS Institute of Information Technology, Lahore, Pakistan for providing us the relevant research facilities.

References

[1] S. Mariethoz, A. Domahidi, and M. Morari, "High-bandwidth explicit model predictive control of electrical drives," *Industry Applications, IEEE Transactions on*, vol. 48, no. 6, pp. 1980–1992, 2012.

[2] M. De Aguiar and M. Cad, "The concept of complex transfer functions applied to the modeling of induction motors," in *Power Engineering Society Winter Meeting, 2000. IEEE*, vol. 1. IEEE, 2000, pp. 387–391.

[3] A. Dumitrescu, D. Fodor, T. Jokinen, M. Rosu, and S. Bucurenciu, "Modeling and simulation of electric drive systems using matlab/simulink environments," in *Electric Machines and Drives, 1999. International Conference IEMD'99*, 1999, pp. 451–453.

[4] O. Ellabban, J. Van Mierlo, and P. Lataire, "Direct torque controlled space vector modulated induction motor fed by a z-source inverter for electric vehicles," in *Power Engineering, Energy and Electrical Drives (POWERENG), 2011 International Conference on*. IEEE, 2011, pp. 1–7.

[5] R. Bojoi, Z. Li, S. A. Odhano, G. Griva, and A. Tenconi, "Unified direct-flux vector control of induction motor drives with maximum torque per ampere operation," in *Energy Conversion Congress and Exposition (ECCE), 2013 IEEE*. IEEE, 2013, pp. 3888–3895.

[6] S. A. Odhano, R. Bojoi, A. Boglietti, S. G. Rosu, and G. Griva, "Maximum efficiency per torque direct flux vector control of induction motor drives," *Industry Applications, IEEE Transactions on*, vol. 51, no. 6, pp. 4415–4424, 2015.

[7] C. Patel, R. P. Day, A. Dey, R. Ramchand, K. Gopakumar, and M. P. Kazmierkowski, "Fast direct torque control of an open-end induction motor drive using 12-sided polygonal voltage space vectors," *Power Electronics, IEEE Transactions on*, vol. 27, no. 1, pp. 400–410, 2012.

[8] K. Hemavathy, N. Pappa, and S. Kumar, "Comparison of indirect vector control and direct torque control applied to induction motor drive," in *Advanced Communication Control and Computing Technologies (ICACCCT), 2014 International Conference on*. IEEE, 2014, pp. 192–197.

[9] E. Ramprasath and P. Manojkumar, "Modelling and analysis of induction motor using labview," *International Journal of Power Electronics and Drive Systems*, vol. 5, no. 3, p. 344, 2015.

[10] A. Hanif, A. I. Bhatti, A. R. Yassin, G. Murtaza, and Q. Ahmed, "Sliding mode-based observer design for field-oriented control of induction machine drive for applications in hybrid electric vehicles," in *Control Conference (CCC), 2014 33rd Chinese*. IEEE, 2014, pp. 263–268.

[11] B. K.Bose, *Modern Power Electronics and AC Drive*. Prentice Hall PTR, 2002.

[12] E. Ramprasath, P. Manojkumar, and P. Veena, "Induction motor analysis using labview," in *Proceeding on International Conference on Electrical Engineering and Technology*, vol. 2, no. 5, 2015, p. 498.

[13] S. Chapman, *Electric machinery fundamentals*. Tata McGraw-Hill Education, 2005.